

$O(a)$ improved Wilson quark action on anisotropic lattice*

T. Umeda^a, H. Matsufuru^b and T. Onogi^b

^aCenter for Computational Physics, University of Tsukuba, Tsukuba 305-8577, Japan

^bYukawa Institute for Theoretical Physics, Kyoto University, Kyoto 606-8502, Japan

The $O(a)$ improved Wilson quark action on the anisotropic lattice is investigated. We carry out numerical simulations in the quenched approximation at three values of lattice spacing ($a_\sigma^{-1} = 1\text{--}2$ GeV) with the anisotropy $\xi = a_\sigma/a_\tau = 4$, where a_σ and a_τ are the spatial and the temporal lattice spacings, respectively. Using the dispersion relation of mesons, the bare anisotropy γ_F in the quark action is numerically tuned below the charm quark mass region with the statistical accuracy of 1 % level. The systematic uncertainties in the calibration are examined and found to be under control in the continuum limit. Then we compute the light hadron masses and find that they are consistent with the result of the UKQCD Collaboration on the isotropic lattice. The effect of the uncertainty in the calibration on the hadron spectrum for physical quark masses is also found to be under control.

1. Introduction

The anisotropic lattice, which allows a finer lattice spacing in the temporal direction, is expected to be useful for physics such as the spectroscopy of exotic states, finite temperature QCD and the heavy quark physics. Since the manifest temporal-spatial axis interchange symmetry is absent, the anisotropy parameters of the action should be tuned by imposing the conditions with which the Lorentz invariance is satisfied for some physical observables. A lot of effort on anisotropic lattices has been devoted to charmonium systems [2–5], but because of the computational cost for calibration, the light quark on the anisotropic has not been explored so far.

In this report, we present our study on the $O(a)$ improved Wilson quark action in the light quark region [1] for the range of quark mass from the massless limit up to around the charm quark mass on the quenched anisotropic lattices with three lattice spacings, $a_\sigma^{-1} = 1\text{--}2$ GeV, at fixed renormalized anisotropy, $\xi = a_\sigma/a_\tau = 4$, where a_σ and a_τ are the spatial and temporal lattice spacings. First the bare anisotropy in the quark action is numerically tuned so that the renormalized fermionic anisotropy is equal to that of the gauge field by imposing the relativistic dispersion

relation of mesons. The systematic uncertainties due to the anisotropy are examined. Then we compute the light hadron spectrum and examine how the uncertainty in the calibration affect the spectrum at the parameters of physical interest. More detailed discussions were presented in [1].

2. Quark action and dispersion relation of free quark

The quark action is the same as the Fermilab action [6] but defined on an anisotropic lattice as has been discussed in Ref. [7]. In the hopping parameter form,

$$S_F = \sum_{x,y} \bar{\psi}(x) K(x,y) \psi(y), \quad (1)$$

$$\begin{aligned} K(x,y) = & \delta_{x,y} - \kappa_\tau \left[(1 - \gamma_4) U_4(x) \delta_{x+\hat{4},y} \right. \\ & \left. + (1 + \gamma_4) U_4^\dagger(x - \hat{4}) \delta_{x-\hat{4},y} \right] \\ & - \kappa_\sigma \sum_i \left[(r - \gamma_i) U_i(x) \delta_{x+\hat{i},y} \right. \\ & \left. + (r + \gamma_i) U_i^\dagger(x - \hat{i}) \delta_{x-\hat{i},y} \right] \\ & - \kappa_\sigma c_E \sum_i \sigma_{4i} F_{4i}(x) \delta_{x,y} \\ & - r \kappa_\sigma c_B \sum_{i>j} \sigma_{ij} F_{ij}(x) \delta_{x,y}, \end{aligned} \quad (2)$$

where κ_σ and κ_τ are the spatial and temporal hopping parameters, r is the Wilson parameter

*Talks presented by T. Umeda and H. Matsufuru.

and c_E and c_B are the clover coefficients. In principle for a given κ_σ , the four parameters $\kappa_\sigma/\kappa_\tau$, r , c_E and c_B should be tuned so that Lorentz symmetry holds up to discretization errors of $O(a^2)$.

In this work, we set the spatial Wilson parameter as $r = 1/\xi$ and the clover coefficients as the tadpole-improved tree-level values, namely,

$$r = 1/\xi, \quad c_E = 1/u_\sigma u_\tau^2, \quad c_B = 1/u_\sigma^3 \quad (3)$$

and perform a nonperturbative calibration only for γ_F . The tadpole improvement [8] is achieved by rescaling the link variable as $U_i(x) \rightarrow U_i(x)/u_\sigma$ and $U_4(x) \rightarrow U_4(x)/u_\tau$, with the mean-field values of the spatial and temporal link variables, u_σ and u_τ , respectively. This is equivalent to redefining the hopping parameters with the tadpole-improved ones (with tilde) through $\kappa_\sigma = \tilde{\kappa}_\sigma/u_\sigma$ and $\kappa_\tau = \tilde{\kappa}_\tau/u_\tau$. We define the anisotropy parameter γ_F as $\gamma_F \equiv \tilde{\kappa}_\tau/\tilde{\kappa}_\sigma$.

For later convenience, we also introduce κ

$$\frac{1}{\kappa} \equiv \frac{1}{\tilde{\kappa}_\sigma} - 2(\gamma_F + 3r - 4) = 2(m_{0\sigma} + 4), \quad (4)$$

where $m_{0\sigma}$ is the bare quark mass in spatial lattice units.

The free quark propagator for the action (2) satisfies the dispersion relation

$$\cosh E(\mathbf{p}) = 1 + \frac{\bar{\mathbf{p}}^2 + (m_0 + \frac{1}{2}\frac{r}{\gamma_F}\hat{\mathbf{p}}^2)^2}{2(1 + m_0 + \frac{1}{2}\frac{r}{\gamma_F}\hat{\mathbf{p}}^2)}, \quad (5)$$

where $\bar{p}_i = \frac{1}{\gamma_F} \sin p_i$, $\hat{p}_i = 2 \sin(p_i/2)$, and $m_0 = m_{0\sigma}/\gamma_F$ is the bare quark mass in temporal lattice units. The rest mass M_1 and the kinetic mass M_2 are defined as $M_1 \equiv E(\mathbf{0})$ and $1/M_2 \equiv \xi^2 d^2 E/dp_i^2|_{\mathbf{p}=\mathbf{0}}$. One can tune the bare anisotropy parameter γ_F so that the rest and kinetic masses give the same values [6]. For small m_0 and with $r = 1/\xi$, this leads the expansion of γ_F in m_0 as

$$\gamma_F^{-1} = \xi^{-1} \left[1 + \frac{1}{3} m_0^2 \right]. \quad (6)$$

The m_0 dependence starts with the quadratic term for $r = 1/\xi$; therefore the dependence on the quark mass is small for sufficiently small m_0 . For example, let us consider the case of $a_\tau^{-1} = 4$ GeV, which corresponds to our coarsest lattice in the simulation. The charm quark mass corresponds

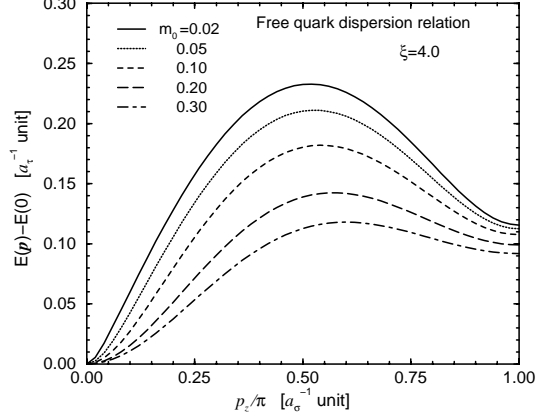


Figure 1. Dispersion relation of the free quark for $\xi = 4$.

to $m_0 \simeq 0.3$ and at this value γ_F is different from ξ by only 3%. Up to this quark mass region, one can expect that the difference of γ_F from ξ will also be small in the numerical simulation.

With our choice, $r = 1/\xi$, the action (2) leads to a smaller spatial Wilson term for a larger anisotropy ξ . The question is whether the contribution of the doubler eliminated by the Wilson term becomes significant for practical value of ξ . Figure 1 shows the dispersion relation (5) for several values of m_0 in the case of $\xi = 4$. Towards the edge of Brillouin zone, the relative energy $E(\mathbf{p}) - E(\mathbf{0})$ rapidly decreases to $\simeq 0.1$ in temporal lattice units. On the other hand, typical energy scale of quarks inside hadrons are about $\Lambda_{QCD} \simeq 200$ MeV for light and heavy-light hadrons. For our coarsest lattice, $a_\tau^{-1} \simeq 4.0$ GeV leads to the doubler's relative energy of about 400 MeV. This seems large enough for eliminating the naive excited state contamination due to the doublers from the ground state signals, although more nontrivial doubler effect such as the shift of energy through the mixing of the ground states and the doubler states is not excluded. Our finest lattice has $a_\tau^{-1} \simeq 8$ GeV which would be sufficiently large to avoid the doubler effect. In the case of heavy quarkonium, typical kinetic energy scale is mv^2 , where v is the quark velocity. For charmonium, $v^2 \sim 0.3$ and typical energy scale is about 300 MeV. Since this is not sufficiently less

than the doubler's relative energy on the lattice of $a_\tau^{-1} \simeq 4.0$ GeV, finer lattices should be used for the charmonium system.

3. Calibration procedures

On an anisotropic lattice, one must tune the parameters so that the anisotropy of quark field, ξ_F , equals that of the gauge field, ξ_G :

$$\xi_F(\beta, \gamma_G; \kappa, \gamma_F) = \xi_G(\beta, \gamma_G; \kappa, \gamma_F) = \xi. \quad (7)$$

Although ξ_G and ξ_F are in general functions of both of gauge parameters (β, γ_G) and quark parameters (κ, γ_F), on a quenched lattice one can determine $\xi_G = \xi$ independently of κ and γ_F , and then tune γ_F so that a certain observable satisfies the condition (7). In this work, we define ξ_F through the relativistic dispersion relation of meson,

$$E^2(\mathbf{p}) = m^2 + \mathbf{p}^2/\xi_F^2 + O[(\mathbf{p}^2)^2], \quad (8)$$

for calibration. In the above expression, the energy and mass E and m are in temporal lattice units while the momentum \mathbf{p} is in spatial lattice units. ξ_F converts the momentum into that in temporal lattice units. For finite lattice spacings, the above dispersion relation only holds up to the $O[(\mathbf{p}^2)^2]$ correction term. In the continuum limit, this higher order term in a would vanish and the relativistic dispersion relation would be restored.

We fit our numerical data for E^2 to the form Eq. (8) and obtain the value of ξ_F for each input value of bare anisotropy γ_F . Then we linearly interpolate ξ_F in terms of γ_F and find γ_F^* , the value of γ_F for which $\xi_F = \xi$ holds.

In order to estimate the systematic errors we also use the dispersion relation that corresponds to the lattice Klein-Gordon action [2],

$$\cosh E(\mathbf{p}) - \cosh E(\mathbf{p} = 0) = \hat{\mathbf{p}}^2/2\xi_{KG}^2. \quad (9)$$

The difference between these two calibration conditions shows the typical size of the lattice discretization errors. Expanding this expression in a , ξ_{KG} is related to ξ_F as

$$\xi_{KG} = \xi_F[1 - m^2/12 + O(a^4)]. \quad (10)$$

The same input γ_F gives a smaller value for ξ_{KG} than ξ_F , and therefore the tuned bare anisotropy γ_F^* results in a larger value in the former case.

Table 1

Lattice parameters. The statistical uncertainty of u_τ is less than the last digit.

β	γ_G	size	a_σ^{-1} [GeV]	u_σ	u_τ
5.75	3.072	$12^3 \times 96$	1.100(6)	0.7620(2)	0.9871
5.95	3.1586	$16^3 \times 128$	1.623(9)	0.7917(1)	0.9891
6.10	3.2108	$20^3 \times 160$	2.030(13)	0.8059(1)	0.9901

4. Numerical Results of Calibration

4.1. Simulation Parameters

Numerical simulations are performed on three quenched lattices with the Wilson plaquette action at $\beta = 5.75, 5.95$, and 6.10 and with the renormalized anisotropy $\xi = 4$. For the values of bare anisotropy of gauge field γ_G , we adopt the relation of γ_G to ξ numerically determined by Klassen in one percent accuracy [9]. Table 1 summarizes the simulation parameters. The configurations are fixed to the Coulomb gauge, which is particularly useful for the smearing of hadron operators.

The lattice cutoffs and the mean-field values of link variables in Table 1 are determined on the smaller lattices with half size in temporal extent for $\beta = 5.75, 5.95$, and otherwise with the same parameters, while at $\beta = 6.10$ the lattice size is $16^3 \times 64$. The lattice cutoffs are determined from the hadronic radius r_0 proposed in [10], by setting the physical value of r_0 as $r_0^{-1} = 395$ MeV. The mean-field values, u_σ and u_τ , are obtained as the average of the link variables in the Landau gauge, where the mean-field values are used self-consistently in the fixing condition [2].

4.2. Quark field calibration

The calibration of the bare anisotropy γ_F in the quark action is performed as described in the last section. The tuned bare anisotropy parameter γ_F^* , at which $\xi_F = \xi$ holds, is determined in the region from strange to charm quark masses using the dispersion relation of the pseudoscalar and vector mesons. The meson energies are extracted from the meson correlators with momenta $\mathbf{p} = \mathbf{n}(2\pi/L)$, where L is the spatial lattice extent and $\mathbf{n} = (0, 0, 0), (1, 0, 0), (1, 1, 0), (1, 1, 1)$, and $(2, 0, 0)$, where we take averages over rotationally

equivalent momenta. The energies are fitted to both linear and quadratic forms in \mathbf{p}^2 in order to obtain ξ_F in each channel, where the linear fit always uses three lowest momentum states. We adopt the result of quadratic fit at $\beta = 6.10$, except for a few lightest quark cases in which the statistical fluctuation in large momentum states is severely large. At $\beta = 5.75$ and 5.95 , linear fit is used in the whole quark mass region, since quadratic fits which include higher momentum states suffer from larger discretization errors.

We measure ξ_F for two to four different values of γ_F . By linear interpolation we find the value of γ_F^* in each channel of PS and V mesons. We take the average of $\gamma_F^*(PS)$ and $\gamma_F^*(V)$ as the central value and use the difference to estimate one of the systematic errors. At each κ , γ_F^* is obtained within 1% statistical error, except for the lightest quark mass region. Figure 2 shows the κ dependence of γ_F^* at $\beta = 6.10$. Similar behaviors are observed on other two lattices. To determine γ_F^* precisely in the light quark mass region and to extrapolate to the chiral limit, we fit γ_F^* to the form

$$\frac{1}{\gamma_F^*}(m_q) = \zeta_0 + \zeta_2 m_q^2, \quad (11)$$

where the quark mass in temporal units m_q is defined as $m_q = \frac{1}{2\xi}(\frac{1}{\kappa} - \frac{1}{\kappa_c})$. The critical hopping parameter κ_c are determined by a linear extrapolation of PS meson mass squared in terms of $1/\kappa$ with two largest κ 's. The result of the fits is listed in Table 2, and represented by the solid line in Figure 2. The linear fit in m_q^2 seems quite successful, and γ_F^* at the chiral limit is close to the tree-level value, ξ . The statistical uncertainty in γ_F^* is estimated to be of the order of 1% for the whole quark mass region. We also carry out a quadratic fit in m_q , as shown in Fig. 2 by the dashed line, and find that the difference in $\gamma_F^*(m_q = 0)$ from the linear fit in m_q^2 is at most 1%. This difference should be considered as the systematic uncertainty in the chiral extrapolation.

4.3. Uncertainties in calibration

To examine the uncertainty in the calibration, the following analyses are also carried out.

(i). We measure the difference between the γ_F^* 's

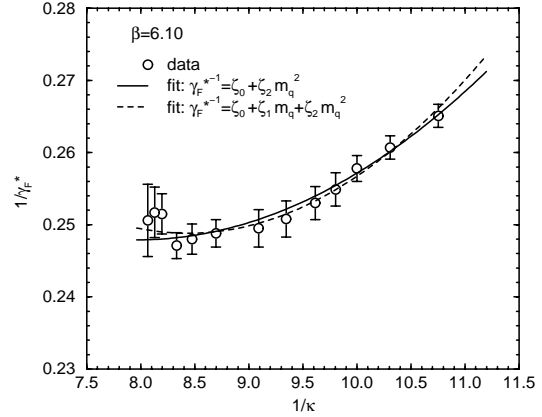


Figure 2. $1/\gamma_F^*$ vs $1/\kappa$ at $\beta = 6.10$. The solid line shows the fit linear in m_q^2 while the dashed line represents the fit quadratic in m_q .

Table 2

Fit results for γ_F^* .

β	ζ_0	ζ_2	κ_c
5.75	0.2558(9)	0.230(12)	0.12640(5)
5.95	0.2490(8)	0.189(15)	0.12592(8)
6.10	0.2479(9)	0.143(14)	0.12558(9)

for the pseudoscalar and vector mesons, which signals the $O(\alpha a)$ systematic error. They tend to decrease towards smaller lattice spacing, and is already consistent with zero at $\beta = 5.95$.

(ii). To estimate the size of $O(a^2)$ systematic uncertainty, γ_F^* is also determined using the lattice Klein-Gordon type dispersion relation, Eq. (9). The results with two dispersion relations come closer to each other by decreasing the lattice spacing. The sizes of this uncertainty in the light quark mass region are 3%, 2%, and 1% for $\beta = 5.75$, 5.85 , and 6.10 , respectively. The behavior in the large quark mass region is consistent with what is expected from Eq. (10).

(iii). We obtain the response of meson masses to a change of γ_F at the fixed κ . The effect of uncertainty in γ_F^* on the meson masses is less than 1%, if γ_F^* is determined at this accuracy. This result is applicable to the relatively heavier quark mass region, such as $m_s < m_q$, and therefore in this region, the errors in the calibration are under

Table 3

Quark parameters used in the hadron spectroscopy. The numbers of configurations are 200 at $\beta = 5.75$ and 100 at $\beta = 5.95$ and 6.10.

β	γ_F	values of κ
5.75	3.909	0.1240, 0.1230, 0.1220, 0.1210
5.95	4.016	0.1245, 0.1240, 0.1235, 0.1230
6.10	4.034	0.1245, 0.1240, 0.1235, 0.1230

control. The light quark mass region is examined in the next section.

5. Light hadron spectroscopy

5.1. Calculation of hadron spectrum

Taking the central value of $\gamma_F = \gamma_F^*$, the light hadron masses are computed in the strange quark mass region $m_s < m_q < 2m_s$ on the same lattices used in the calibration, while with smaller statistics. The parameters are listed in Table 3. In this region, we regard that m_q is sufficiently small and adopt the value of γ_F^* in the massless limit.

The quark propagators are smeared at the source with Gaussian smearing function with the deviation $\simeq 0.4$ fm, in the Coulomb gauge. For baryons, two of the quarks are set to have degenerate masses.

In order to avoid the ambiguities in the definition of the quark mass, we extrapolate the hadron masses to the chiral limit in terms of the pseudoscalar meson mass squared, instead of $1/\kappa$. We assume the relation

$$m_{PS}^2(m_1, m_2) = B(m_1 + m_2); \quad (12)$$

so that $m_{PS}^2 = 2Bm_1$ holds for the degenerate quark masses, $m_1 = m_2$. Instead of m_i ($i=1,2$), one can use $m_{PS}(m_i, m_i)^2$ as the variable in the chiral extrapolation. For vector mesons and octet and decuplet baryons, we also use the linear relations. The linear fit looks successful.

5.2. Spectrum at physical quark masses

We compare our hadron spectrum at the physical quark masses with the result in the continuum limit by UKQCD Collaboration on an isotropic lattice [11]. We do not extrapolate our data to the continuum limit for lack of the number of different β 's as well as the statistical accuracy. We

adopt two different inputs to set the scale: one is hadronic radius r_0 and the other is the K^* meson mass, which were also adopted in [11]. From each of these scales the physical u , d and s quark masses are determined respectively. (We do not distinguish the u and d quark masses.)

While we show only the result with the scale set by r_0 , similar result is obtained with the scale set by K^* meson mass. The hadron masses extrapolated or interpolated to the physical points are shown in Figure 3, together with the results of UKQCD in the continuum limit. In our data, differences between the results at $\beta = 6.10$ and 5.95 are rather large compared with the difference between $\beta = 5.95$ and 5.75. This could be partially due to the different a dependence of $O(\alpha a)$ and $O(a^2)$ lattice artifacts, and also due to the statistical fluctuation. Our results of the hadron masses seem to approach the continuum results by UKQCD Collaboration on an isotropic lattice. We also compare the parameter J ,

$$J = \left. \frac{m_V dm_V}{dm_{PS}^2} \right|_{m_V/m_{PS}=m_{K^*}/m_K}, \quad (13)$$

which was introduced to probe the quenching effect [12]. It is known that the quenched lattice simulation does not reproduce the experimental value, $J = 0.48(2)$, and gives about 20% smaller value. Our results are consistent with those of UKQCD on isotropic lattices in the quenched approximation, as shown in Fig. 3.

5.3. Systematic errors of the spectrum from calibration

To estimate the effect of the uncertainty of calibration on the spectrum, we obtain the spectrum at the same κ 's with slightly shifted bare anisotropy, $\gamma_F' = \gamma_F^* + \delta\gamma_F$. We set $\delta\gamma_F = 0.1$, which implies about 2.5 % shift of bare anisotropy. The difference between the masses with γ_F' and γ_F^* is slightly amplified toward the chiral limit. Even for the lightest mass in each hadron species, the difference is at most around 1%. This implies that the uncertainty of hadron masses at the physical (u, d) and s quark masses are about half the uncertainty in γ_F . With the relativistic dispersion relation, γ_F^* at $m_q = 0$ has been determined at each β within about 2% am-

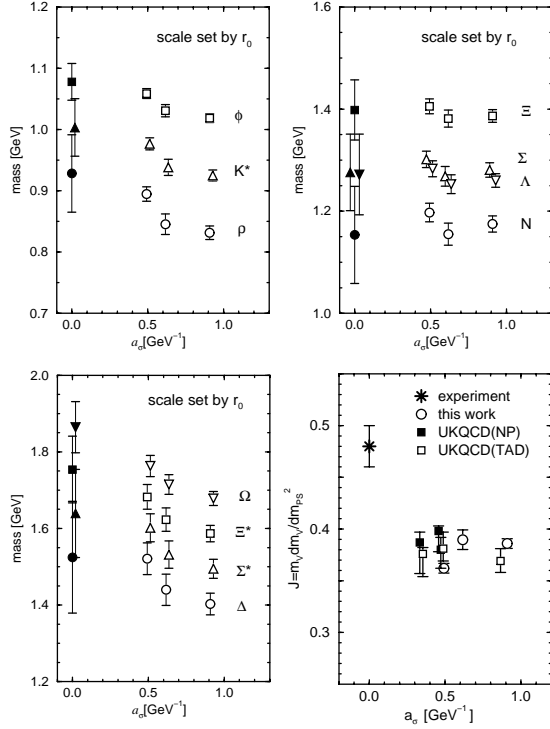


Figure 3. Hadron masses and the parameter J . The a_σ is set by using r_0 . Filled symbols are the results of UKQCD Collaboration on the isotropic lattices [11].

biguity: the statistical error of 1 % and the systematic error of 1 % in the form of fit. Therefore there is 1 % level uncertainty in the hadron spectrum due to the uncertainty in calibration. This feature makes the anisotropic lattice promising for future physical applications.

6. Conclusion

We studied the $O(a)$ improved quark action on the anisotropic lattice with anisotropy $\xi = a_\sigma/a_\tau = 4$. The bare anisotropy γ_F^* , with which $\xi_F = \xi$ holds, is determined for the whole quark mass region below the charm quark mass, including the chiral limit, in 1 % statistical accuracy. In the massless limit, there is also about 1 % systematic uncertainty in extrapolating γ_F^* to $m_q = 0$. We estimate the typical sizes of $O(\alpha a)$ and $O(a^2)$ systematic uncertainties as to be 4% at $\beta = 5.75$

and smaller for larger β . We then calculated the light hadron spectrum and found a consistent result with previous work on an isotropic lattice by UKQCD. The relative errors in hadron spectrum for physical quark masses are half of those in γ_F^* . Since finite lattice spacing errors tend to vanish as a decreases, we expect to obtain the hadron spectrum in the continuum limit within 1% uncertainty due to the anisotropy. This encouraging results suggest that the anisotropic lattice would already be applicable to quantitative studies of a few percent accuracy. To achieve higher accuracy, nonperturbative tuning of the clover coefficients is required.

The simulation was done on a NEC SX-5 at RCNP, Osaka University and a Hitachi SR8000 at KEK. H.M. thank JSPS for Young Scientists for financial support. T.O. is supported by Grants-in-Aid of the Japanese Ministry of Education (No. 12640279).

REFERENCES

1. H. Matsufuru, T. Onogi and T. Umeda, hep-lat/0107001, to appear in Phys. Rev. D.
2. T. Umeda, R. Katayama, O. Miyamura and H. Matsufuru, Int. J. Mod. Phys. A **16** (2001) 2215.
3. T. R. Klassen, Nucl. Phys. B (Proc. Suppl.) **73** (1999) 918.
4. P. Chen, Phys. Rev. D **64** (2001) 034504.
5. CP-PACS Collaboration, A. Ali Khan *et al.*, Nucl. Phys. B (Proc. Suppl.) **94** (2001) 325.
6. A. X. El-Khadra, A. S. Kronfeld and P. B. Mackenzie, Phys. Rev. D **55** (1997) 3933.
7. J. Harada, A. S. Kronfeld, H. Matsufuru, N. Nakajima and T. Onogi, Phys. Rev. D **64** (2001) 074501.
8. G. P. Lepage and P. B. Mackenzie, Phys. Rev. D **48** (1993) 2250.
9. T. R. Klassen, Nucl. Phys. B **533** (1998) 557.
10. R. Sommer, Nucl. Phys. B **411** (1994) 839.
11. UKQCD Collaboration, K. C. Bowler *et al.*, Phys. Rev. D **62** (2000) 054506.
12. UKQCD Collaboration, P. Lacey and C. Michael, Phys. Rev. D **52** (1995) 5213.